Virologica Sinica 37 (2022) 601–609

Contents lists available at ScienceDirect

Virologica Sinica

journal homepage: www.keaipublishing.com/en/journals/virologica-sinica
www.virosin.org

Research Article

Growth hormone attenuates the brain damage caused by ZIKV infection in mice

Zi-Da Zhen [a,1], Na Wu [b,1], Dong-Ying Fan [a], Jun-Hong Ai [a], Zheng-Ran Song [a], Jia-Tong Chang [a], Pei-Gang Wang [a], Yan-Hua Wu [a,*], Jing An [a,*]

[a] Department of Microbiology, School of Basic Medical Sciences, Capital Medical University, Beijing, 100069, China
[b] Laboratory Animal Resource Center, Capital Medical University, Beijing, 100069, China

ARTICLE INFO

Keywords:
Zika virus (ZIKV)
Growth hormone
Apoptosis
Microcephaly

ABSTRACT

As a member of vector-borne viruses, Zika virus (ZIKV) can cause microcephaly and various neurological symptoms in newborns. Previously, we found that ZIKV could infect hypothalamus, causing a decrease in growth hormone (GH) secretion, growth delay and deficits in learning and memory in suckling mice. Early administration of GH can improve the cognitive function of the mice. Therefore, in this study we further investigated the mechanism underlying the protective role of GH in ZIKV infection in suckling mice. Our results showed that GH could effectively reduce brain damage caused by ZIKV infection via reducing cell apoptosis and inflammatory response rather than inhibiting viral replication. Our results provide important evidences not only for understanding the mechanism underlying ZIKV-associated neurological symptoms but also for the treatment of ZIKV infection.

1. Introduction

Zika virus (ZIKV) belongs to the *Flaviviridae* family and is transmitted mainly by mosquitoes, and also by non-vector transmission including maternal-fetal and sexual routes. ZIKV infection during pregnancy is associated with severe brain development defects in fetus, including microcephaly, neurodevelopmental abnormality and other serious congenital neurological complications (Xu et al., 2019), known as congenital Zika syndrome. Adults infected with ZIKV also have neurological complications such as Guillain-Barré syndrome (Figueiredo et al., 2019). In the fetal, neural progenitor cells are important target cells of ZIKV (Gabriel et al., 2017). Further studies found that ZIKV could infect different types of neurons and replicate effectively in the brain of embryonic mice, causing damage to neurons in the hippocampus and impairing the synaptic function and memory function (Figueiredo et al., 2019). ZIKV infection leads to cortical thinning and microcephaly through causing cell cycle arrest, inducing their premature differentiation, inhibiting the proliferation of neural cells, and activating the apoptosis of neural progenitor cells (Li et al., 2016; Liu et al., 2018; Ferraris et al., 2019). Therefore, it is speculated that neuron apoptosis caused by ZIKV is not only an important mechanism underlying pathological damage of brain but also is one of the possible targets for ZIKV therapeutic strategy. In previous studies, we found that ZIKV could infect the hypothalamus of suckling mice and lead to growth delay and memory impairment through affecting neuroendocrine function of the hypothalamus-pituitary-thyroid axis. Early administration of growth hormone (GH) can improve the growth, development and alleviate the cognitive impairment in mice (Wu et al., 2018). GH plays an important role for body development. Meanwhile, it has been reported that GH can inhibit cell apoptosis in many types of cells and reduce inflammation and pathological damage (Svensson et al., 2008; Keane et al., 2015; Lindboe et al., 2016; Tian et al., 2017; Liu et al., 2019; Gong et al., 2020; Wang et al., 2021). However, most of the previous studies have focused on the role of GH in non-infectious conditions, but the role of GH in ZIKV infection remains unclear. Therefore, we investigated whether GH treatment protects against brain injury by inhibiting apoptosis and reducing inflammation caused by ZIKV infection, and the mechanism underlying this phenomenon.

In this study, we compared the growth and pathological changes of brain between ZIKV infected and ZIKV infection with GH treated mice. We found that administration of GH not only improved body weight but also enhanced the survival rate of ZIKV infected mice via reducing

* Corresponding authors.
E-mail addresses: wuyanhua@ccmu.edu.cn (Y.-H. Wu), anjing@ccmu.edu.cn (J. An).
[1] Zi-Da Zhen and Na Wu contributed equally to this work.

https://doi.org/10.1016/j.virs.2022.06.004
Received 15 January 2022; Accepted 10 June 2022
Available online 15 June 2022

inflammation and pathological damage. These results indicate that GH can play a neuroprotective role in ZIKV infection.

2. Materials and methods

2.1. Virus and cells

ZIKV (Asian strain, SMGC-1 strain) was isolated from Zika fever patients and kindly provided by Dr. George F. Gao (Institute of Microbiology, Chinese Academy of Sciences, Beijing, China). C6/36 (Aedes albopictus cells) cells were maintained at 28 °C in RMPI 1640 (61870036, Gibco, USA) with 10% fetal bovine serum (FBS, 10099, Gibco, USA). Vero cells (African green monkey kidney cells) were maintained in MEM (12492013, Gibco, USA) with 5% FBS at 37 °C and 5% CO_2. HT-22 (murine hippocampal neuronal cells) cells were maintained at 37 °C in DMEM (11995123, Gibco, USA) with 10% FBS. ZIKV was propagated in C6/36 cells and stored at −80 °C. Virus titers were determined by plaque assay on Vero cells under overlay medium containing 1% methylcellulose and 5% FBS in MEM. The plaques were visualized by staining with crystal violet solution, and were then counted (Wang et al., 2017).

2.2. Animal experiment

BALB/c mice were purchased from the Academy of Military Medical Sciences (Beijing, China) and type I interferon receptor deficient ($ifnar^{-/-}$ A6) mice were provided by the Institute of Laboratory Animals Science, Peking Union Medical College. All mice were maintained in specific pathogen-free animal facility. In suckling BALB/c mouse group, one-day suckling BALB/c mice were divided into four sub-groups (5–10 mice for each sub-group): ZIKV + GH, GH, ZIKV, and phosphate buffered solution (PBS). Following intracerebral (i.c.) infection with 100 PFU ZIKV in a 20 μL volume, mice were then administered a dose of 6 μg/g of recombinant human GH (Recombinant Human Growth Hormone Injection, S20050024, China) or an equal volume of PBS as a control via subcutaneous injection once per day in the following 7 day as previously reported (Wu et al., 2018). Survival rate and weight were tracked for 28 days.

In adult mouse group, 8-week A6 mice of either gender were injected intraperitoneally (i.p.) with 1000 PFU (for observing symptoms) or 2000 PFU (for survival rate and body weight) of ZIKV in 100 μL of PBS and followed by GH administration daily for seven days. On 9 days post-infection (dpi), main organs (brain, liver, spleen, kidney) and blood of the mice were collected for examining pathological changes and viral load.

2.3. Quantitative RT-PCR (qRT-PCR)

The qRT-PCR is used for detecting viral load in the main organs (brain, liver, spleen, kidney) and blood. In brief, RNA was extracted from the tissue or serum, and dissolved in RNase-free water Transzol (ET101-01, TransGen, China) according to the manufacturer's protocol. Quantitative RT-PCR was performed on the 7500 Real Time PCR System (Applied Biosystems, USA) using the Quant One Step qRT-PCR kit (FP303-01, Tiangen, China) as previously reported (Wu et al., 2018). Primer sequences are shown in Supplementary Table S1. The quantification of ZIKV mRNA copies is determined by the standard curve method and expressed as the copy number per μg total RNA (for organs) or mL (for sera) (Wang et al., 2017). Relative quantification of *BAX* and *Bcl*-2 mRNA was determined by using *GAPDH* as internal control and $2^{-\Delta\Delta Ct}$ method.

2.4. Immunofluorescence (IF) staining and TdT-mediated dUTP nick end labeling (TUNEL) staining

Brain was immediately embedded in opti-mum cutting temperature compound (OCT, 4583, SAKURA, USA), and then frozen sections with 5 μm thickness were made. After being air-dried and then fixed in 4% paraformaldehyde (PFA), the tissue sections were treated with 0.5% Triton-X100 (93,443, Sigma, USA) solution and blocked in 1% bovine serum albumin (BSA, BSAV-RO, Sigma, USA). Then sections were either subjected to IF or TUNEL staining. For IF staining, sections were incubated with primary antibodies to ZIKV (antibody 4G2, diluted 1:1000), to NeuN (ab104225, Abcam, USA, diluted 1:500), to cleaved caspase-3 (9664s, CST, USA, diluted 1:500), or to cleaved caspase-1 (AF4022, Affinity, USA, diluted 1:500) at 4 °C overnight, and followed by incubation with goat anti-mouse IgG Alexa Fluor 488 (A-11029, Invitrogen, USA, diluted 1:500) or goat anti-rabbit IgG Alexa Fluor 594 (R37117, Invitrogen, USA, diluted 1:500). For TUNEL staining, sections were incubated with the TUNEL staining solution of Beyotime Apoptosis TUNEL Kit (c1088, Beyotime, China) at 37 °C for 1 h, according to the manufacturer's manual. The section was observed and images were captured with a laser scanning confocal microscope (Leica TCS SP5, Germany).

2.5. Immunohistochemical (IHC) and hematoxylin and eosin (HE) staining

Tissues from main organs were immediately fixed in 4% PFA and then embedded in paraffin. Sections (5 μm) were stained with HE according to standard methods. For IHC staining, the sections were baked at 60 °C for 30 min and were then deparaffinized by xylene, absolute ethanol, 75% ethanol, and boiled in citrate buffer for antigen retrieval. Then, the sections were incubated with antibodies to CD4 (ab183685, Abcam, diluted 1:500) or to CD8 (98941S, CST, diluted 1:500). Samples were counterstained nucleus with hematoxylin (G1080, Solarbio, China).

2.6. Western blotting

The protein level of cleaved caspase-3 in mouse brain was measured by Western blotting. In brief, the brain samples collected at 9 dpi were homogenized on ice in lysis buffer containing a complete protease and phosphatase inhibitor cocktail (23,227, Thermo Scientific, USA). After being centrifuged, the samples were separated using 10% sodium dodecyl sulfate polyacrylamide gel electrophoresis (SDS-PAGE) and transferred to PVDF membranes (ISEQ00010, Millipore, USA). The membranes were blocked with TBS buffer containing 10% skim milk and incubated with primary antibodies to cleaved caspase-3 (9664s, CST, diluted 1: 1000) or to β-actin (HC201-01, TransGen, China, diluted 1: 1000) overnight at 4 °C. As the secondary antibody, goat anti-rabbit IgG or donkey anti-mouse IgG (926–68071 or 925–32212, LI-COR, USA, diluted 1: 5000) was added and the protein band was visualized by using an infrared laser imager 767 (Odyssey® CLX, USA).

2.7. Flow cytometry

At 9 dpi, cerebral cortex of mice was collected and then treated with digestion solution containing 0.25% trypsin and 0.02% EDTA in PBS for 30 min at 37 °C. An equal volume of 10% FBS in DMEM was added and the supernatant was filtered with a 200-mesh filter. After centrifugation and resuspension, the cells were fixed with 4% PFA and followed with incubation with antibody to cleaved caspase-3 (9664s, CST, diluted 1:250) for 1 h at room temperature. Then goat anti-mouse IgG Alexa Fluor 488 (A-11029, Invitrogen, 1:500) was added and incubated for 30 min. The flow cytometry was performed on a DxFLEX flow cytometer (Beckman Coulter, USA) and followed by analyzing with CytExpert software (version 2.0).

2.8. Statistical analysis

Statistical analysis was performed on GraphPad Prism 7.0 software. Student's *t*-test, Welch's correction and Mann-Whitney test were used to

compare quantitative data between two groups. Analysis of variance (ANOVA) and multiple *t*-tests were used to compare grouped quantitative data. When the *P* value is < 0.05, the comparison is considered to be statistically different.

3. Results

3.1. GH treatment improves survival rate and body weight of suckling mice

To study the role of GH in ZIKV infection, one-day suckling mice were i.c. injected with ZIKV then treated with GH or i.c. injected with PBS as control. As shown in Fig. 1A and B, in ZIKV infection group, the body weight and body length of the mice were both less than that of the mice in PBS control group, indicating that ZIKV infection caused growth delay. However, in ZIKV + GH group, GH treatment improved growth delay and enhanced survival rate compared with that in ZIKV infection group. The survival rates of ZIKV group was only 40% (4/10), while that of ZIKV + GH group was 80% (8/10, Fig. 1C). Consistently, the death time of the mice was also postponed by administration of GH, suggesting that GH improved the growth and survival of ZIKV infected suckling mice. The results showed that GH had a definite protective effect on suckling mice during ZIKV infection.

3.2. GH does not inhibit ZIKV replication in vivo and in vitro

Next, to understand mechanism underlying the protection of GH, we tested the effect of GH on ZIKV replication. One-day suckling mice were i.c. injected with ZIKV then treated with GH or i.c. injected with PBS as control. At 9 dpi, mice brain, liver, spleen and kidney were collected for detecting viral load. As shown in Fig. 2A, in ZIKV infection group, the viral load in the mouse brain was about $10^{5.7}$ copies per μg total RNA, while in liver, spleen, and kidney, the viral load was lower than that in the brain tissue, which were $10^{1.8}$, $10^{2.6}$, $10^{3.3}$ copies/μg total RNA. There was no significant difference in the viral load of each tissue between the ZIKV group and the ZIKV + GH group (Fig. 2A). Meanwhile, HT-22 cells were used to detect the effect of GH on ZIKV replication *in vitro*. Firstly, the expression of GH receptor on the HT-22 cells was confirmed by qRT-PCR. Then we detected the ZIKV RNA loads in the cell supernatant at 12 h and 24 h after ZIKV infection. The viral load in the ZIKV group was $10^{3.2}$ and $10^{4.3}$ copies per mL of cell supernatant at 12 h and 24 h, respectively. There was no significant difference in the number of virus copies between the ZIKV + GH treatment group and the ZIKV group (Fig. 2B). These results indicated that GH had little effect on the replication of ZIKV *in vivo* and *in vitro*. In other words, GH protected mice from ZIKV infection potentially via other way but not by inhibiting ZIKV replication.

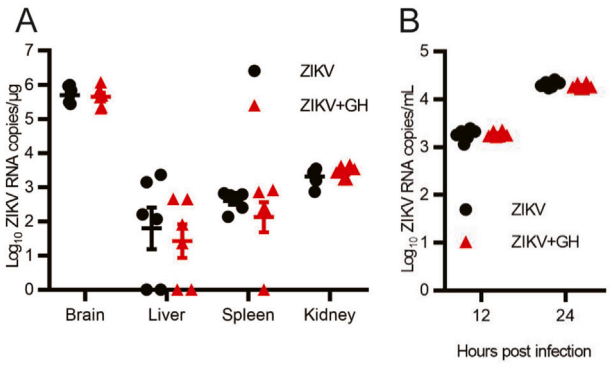

Fig. 2. Effects of GH on the replication of ZIKV *in vitro* and *in vivo*. **A** Viral load in brain, liver, spleen, kidney of suckling mice intracerebrally injected with 100 PFU ZIKV within 24 h after birth at 9 dpi. Each dot denotes a mouse. **B** Viral load in supernatants of HT-22 cells infected with ZIKV (MOI = 1) at different time points. All the data are expressed as the means ± SEM. Statistical analysis was performed by student *t*-test. CTRL, control; GH, growth hormone; ZIKV, Zika virus; SEM, standard error of mean.

3.3. GH treatment can reduce the pathological damage caused by ZIKV in mouse brain

Because brain is a major target organ for ZIKV, we detected pathological changes in infected mouse brain after treatment with GH. As shown in Fig. 3A, the size of mouse brain in ZIKV + GH group was obviously larger than that in ZIKV group, and GH treatment increased the average weight of the brain from 0.27 g to 3.2 g (Fig. 3B). By HE staining, obvious pathological changes, including denaturation and loss of neurons and infiltration of inflammatory cell in hippocampus, cerebral cortex and cerebellum were observed in ZIKV group (Fig. 3C). The brain tissue of the ZIKV + GH group had similar pathological changes of that in ZIKV group, but the degree of the lesions was significantly weakened, manifested as the loss of neurons in the cortex and hippocampus, and the reduction of vacuoles degeneration. The structure of the cerebellum was relatively intact and the cell density was significantly higher than ZIKV group after GH treatment. We counted lesion cells in each region of the mouse brain, and the number of lesion cells in cortex, hippocampus and cerebellum in ZIKV group were 61.8 ± 17.4, 59.2 ± 8.6, 243.7 ± 76.4 cells per high power field (HPF), respectively. As for ZIKV + GH group, the number of lesion cells was 16.8 ± 5.1, 22.7 ± 4.8, 77.8 ± 30.3, which was significantly less than that in ZIKV group (Fig. 3D–F). The viral antigen in brain was also detected, and we found neurons were the mainly target cells in both ZIKV group and ZIKV + GH group (Fig. 3G), indicating that GH

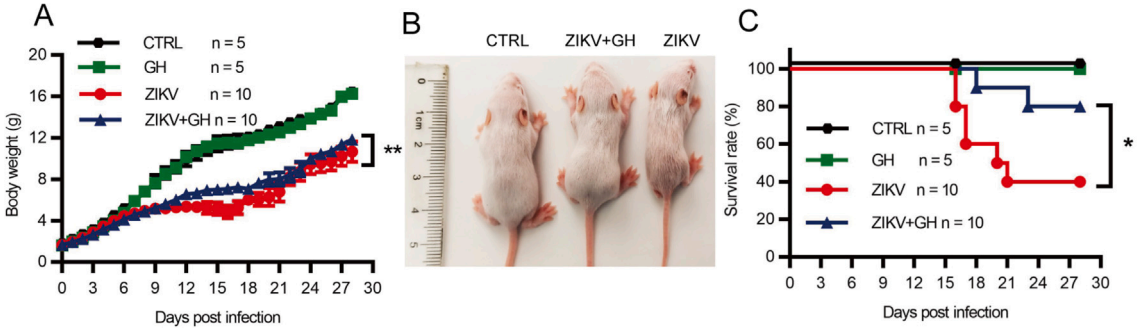

Fig. 1. Effects of GH on body weight and survival of ZIKV-infected suckling mice. **A** Changes of body weight of suckling mice intracerebrally injected with 100 PFU ZIKV within 24 h after birth. GH was given daily for the first 7 days at 6 μg/g body weight (n = 10 for ZIKV and ZIKV + GH group, n = 5 for GH and CTRL group). Data are expressed as means ± SEM. Statistical analysis was performed by two-way ANOVA. **B** Representative photo of mice at 9 dpi. **C** Survival rate of suckling mice. Statistical analysis was performed by log-rank test. $^*P < 0.05$, $^{**}P < 0.01$. CTRL, control; GH, growth hormone; ZIKV, Zika virus; SEM, standard error of mean.

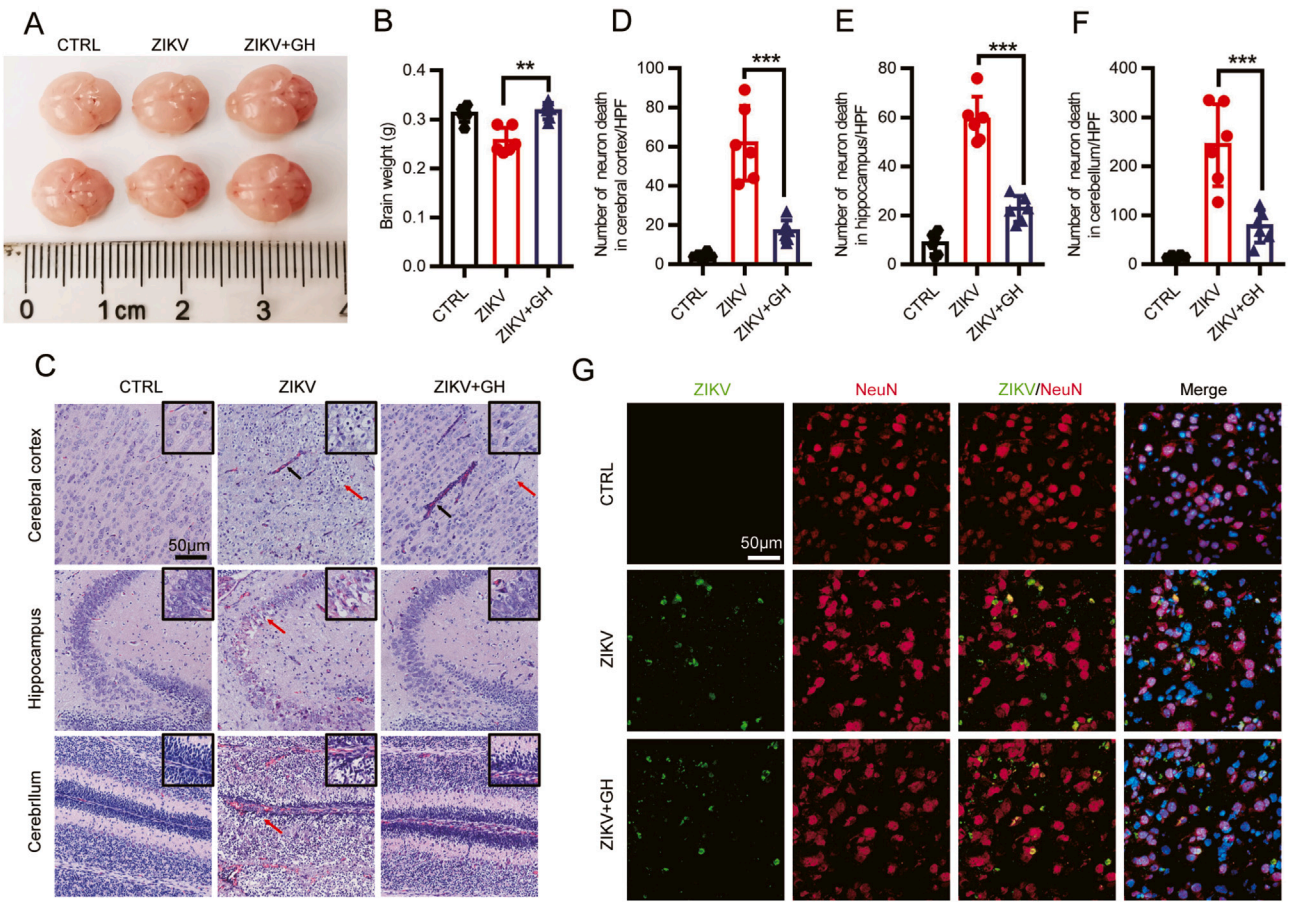

Fig. 3. GH reduced the pathological changes in mouse brain caused by ZIKV infection. Representative image of brain (**A**) and brain weight (**B**) of suckling mice intracerebrally injected with 100 PFU ZIKV after birth. **C** Hematoxylin eosin staining of cerebral cortex, hippocampus and cerebellum at 9 dpi. Red arrows are cell loss, black arrows are inflammatory cell infiltration. **D–F** Number of neuron death in cerebral cortex, hippocampus and cerebellum per high power field (HPF). **G** Immunofluorescent co-staining of ZIKV antigen (green) and neural cell marker (red) in the brain. DAPI (blue) denotes nucleus. All the data are expressed as the means ± SEM. Each dot represents a mouse. Statistical analysis was performed by student *t*-test. $^{**}P < 0.01$, $^{***}P < 0.01$. CTRL, control; GH, growth hormone; ZIKV, Zika virus; SEM, standard error of mean.

treatment did not change the cell tropism of ZIKV. Taken together, the results suggested that GH alleviated the pathological damage of brain neither by affecting the ZIKV replication nor changing the cell tropism. To observe the effect of GH on the long-term pathological changes, we performed HE staining on the brain tissue at 8 weeks after infection when ZIKV RNA could not be detected. In contrast to obvious histopathological changes in the cortex of mouse brain in ZIKV group, GH treatment could also alleviate the degree of the pathological lesion observed at 8 weeks after infection (Supplementary Fig. S1).

3.4. GH treatment can reduce lymphocyte infiltration in mouse brain tissue

In ZIKV group, numerous $CD8^+$ T cells were detected in neonatal mouse brain, and GH treatment significantly reduced the infiltration of $CD8^+$ T lymphocytes in neonatal mouse brain, reducing average number of $CD8^+$ T cells from 45 to 20 per HPF (Fig. 4A–C). Similarly, GH treatment could also reduce the infiltration of $CD4^+$ T cells although there was slight infiltration in brain tissue (Fig. 4D–F). The results indicated that GH treatment reduced the lymphocyte infiltration in the brain of mice.

3.5. GH treatment reduces neuronal apoptosis in mouse brain tissue

Next, the characteristics of neuronal death induced by ZIKV were investigated. By IHC, all pyroptosis, autophagy and apoptosis were observed in mouse brain. Of those, neuronal apoptosis was particularly prominent. Therefore, we tested the effect of GH treatment on the apoptosis in mouse brain. The mRNA levels of *Bax* and *bcl-2* in mouse brain tissue after ZIKV infection were significantly changed. *Bax,* a pro-apoptotic protein, was significantly upregulated in ZIKV group, which was up to 2.5-fold higher than that in ZIKV + GH group. *Bcl-2,* an anti-apoptotic protein, was significantly down-regulated in ZIKV group, only 0.5 times of that in ZIKV + GH group (Fig. 5A). Furthermore, we analyzed the protein level of cleaved caspase-3 in mouse brain by Western blotting. The obvious activation of caspase-3 was observed in ZIKV infected mouse brain. However, GH treatment significantly reduced caspase-3 activation (Fig. 5B). The gray density of the caspase-3 band was only 0.2 times of that in ZIKV group (Fig. 5C). This result was further supported by IF staining. Compared to ZIKV group, decreased cleaved caspase-3-positive cells were detected in mouse brain of ZIKV + GH group, indicating the inhibitory effect of GH on apoptosis (Fig. 5D and E). Consistently, the apoptosis cells in mouse brain were significantly reduced by GH treatment as shown by the TUNEL staining (Fig. 5F and G) and flow cytometry analysis (Fig. 5H and I). Taken together, all the results showed that GH treatment inhibited the activation of caspase-3 and cell apoptosis in mouse brain.

3.6. GH alleviates brain damage in ZIKV infected adult mice

To study whether GH treatment can also improve the brain damage induced by ZIKV in adult mice, 8-week old A6 mice were i.p. injected with ZIKV. As shown in Fig. 6, there was no significantly difference in body weight of mice between ZIKV group and ZIKV + GH group (Fig. 6A).

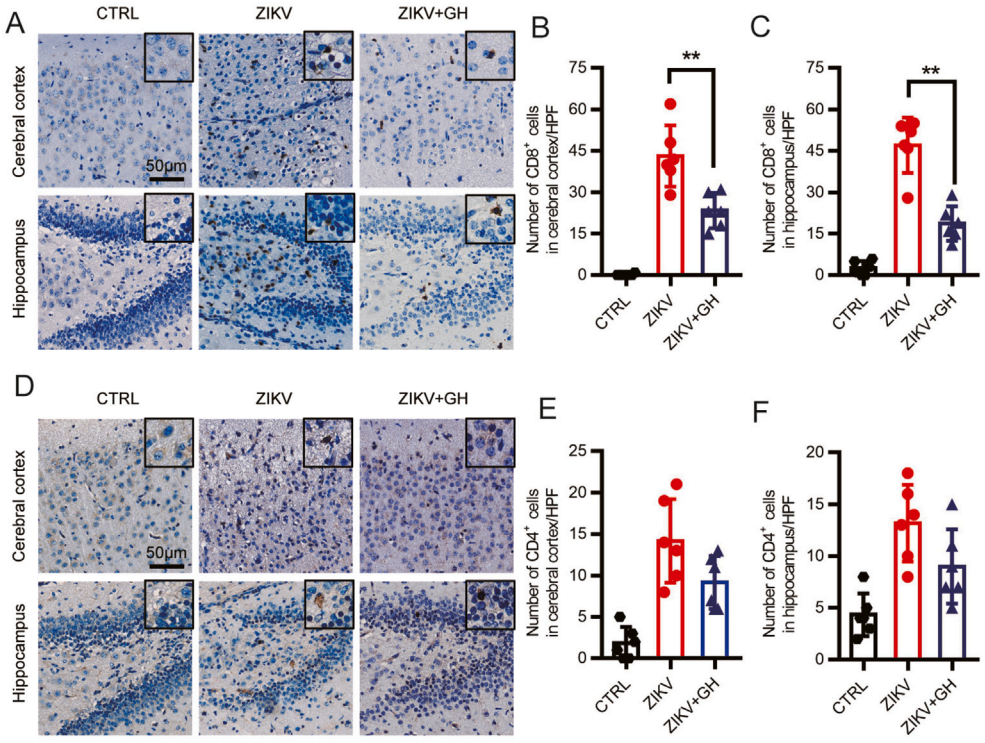

Fig. 4. T lymphocytes infiltration in the brain during ZIKV infection. **A** Representative IHC image depicting $CD8^+$ T cells. **B–C** Quantitative analysis of the number of $CD8^+$ T cells infiltration in brain at 9 dpi. **D** Representative IHC image depicting $CD4^+$ T cells. **E–F** Quantitative analysis of the number of $CD4^+$ T cells per high power field (HPF) in brain at 9 dpi. All the data are expressed as the means ± SEM. Each dot represents a mouse. Statistical analysis was performed by student *t*-test. $^{**}P < 0.01$. CTRL, control; GH, growth hormone; ZIKV, Zika virus; SEM, standard error of mean.

The survival rate of ZIKV group was 50% (3/6), while that of ZIKV + GH group was 66.7% (4/6, Fig. 6B). Meanwhile, slight clinical symptoms with faster recovery were also observed in ZIKV + GH group in comparison to that in ZIKV group (Fig. 6C). By HE staining, in ZIKV group, obvious pathological changes were observed in the brain including hyperemia, neuron death and infiltration of inflammatory cells in hippocampus and cerebral cortex. As expected, GH treatment alleviated the above brain damages (Fig. 6D). IHC also showed that GH treatment reduced $CD8^+$ T cell infiltration in brain tissue in adult mouse (Fig. 6E). After GH treatment, $CD8^+$ T cells decreased from 59 per HPF to 39 per HPF in the cortex and from 50 per HPF to 28 per HPF in the hippocampus (Fig. 6F and G). However, unlike in suckling mice, there was no significant increase in $CD4^+$ cells in the brain tissue of mice after ZIKV infection (Fig. 6H). Compared with the ZIKV group, the activation of caspase-3 in the brain tissue of the mice in the ZIKV + GH group was also reduced by half (Fig. 6I and J). The results suggested that GH also had similar effect on adult mice. However, the protective effect was slightly weaker than that in suckling mice, which may be due to the decreased level of GH receptor in adult mouse brain (Supplementary Fig. S2).

4. Discussion

It was reported that ZIKV infection could cause congenital Zika syndrome via inducing apoptosis and autophagy in cortical progenitor cells and impairing the development of brain (Cugola et al., 2016; Dang et al., 2016). However, the treatment strategies against ZIKV infection in nervous system are very limited. In previous studies, we found that ZIKV infection in suckling mice caused a decreased GH level and growth delay, which could be improved by the administration of GH in the early stage of ZIKV infection (Wu et al., 2018). By using human umbilical vein endothelial cells (HUVEC), it was also found that ZIKV infection could significantly down-regulate GH expression at the transcription level (Khaiboullina et al., 2019). It is reported that as an anti-apoptotic factor, GH has a profound protective effect on neuron damage in the nervous system and promotes cell proliferation and differentiation. Therefore, GH is closely associated with a variety of behaviors, cognitive functions, neurotransmission and neuroendocrine (Aramburo et al., 2014). To investigate its effect on brain damage induced by ZIKV infection, GH was injected subcutaneously into ZIKV infected mice in this study. We found that GH treatment could alleviate the pathological changes in mouse brain including significantly reduced inflammatory cell infiltration and cell apoptosis. Our results proved the protective effect of GH on the central nervous system of ZIKV infected mice.

The mechanism underlying ZIKV-induced brain damage improved by GH treatment is not fully elucidated. In fact, the pathogenesis of ZIKV infection is a complex virus-host response, which is linked to a variety of host genes and signaling pathways. In the central nervous system, ZIKV infection induces apoptosis of neurons via the activating caspase-3/7, -8, and -9 and inhibiting the expression of *Bcl 2*, an antiapoptosis gene (Lee et al., 2020). In addition, ZIKV non-structural protein 4B (NS4B) induces apoptosis by regulating the activation of pro-apoptotic protein Bax (Han et al., 2021). ZIKV induces p53-mediated apoptosis in human neural progenitor cells via interacting with p53 (Li P. et al., 2021). ZIKV infection may initiate the early activation of the Notch pathway, leading to abnormal cell proliferation, apoptosis and differentiation expression (Ferraris et al., 2019). ZIKV also inhibits STAT5 activation and blocks STAT5 signaling by NS4A (Zimmerman et al., 2019). Taken together, ZIKV-induced brain damage is related to a variety of signaling pathways, and these involved molecules may be the target sites of therapy for ZIKV infection. Both exogenous GH and autocrine GH from hippocampal subgranular zone cells can promote the proliferation and survival of hippocampal subgranular zone neurospheres (Devesa et al., 2014). GH treatment can promote the activation of Akt-mTOR and JNK signaling pathways. Blocking these pathways can reduce or eliminate GH effects,

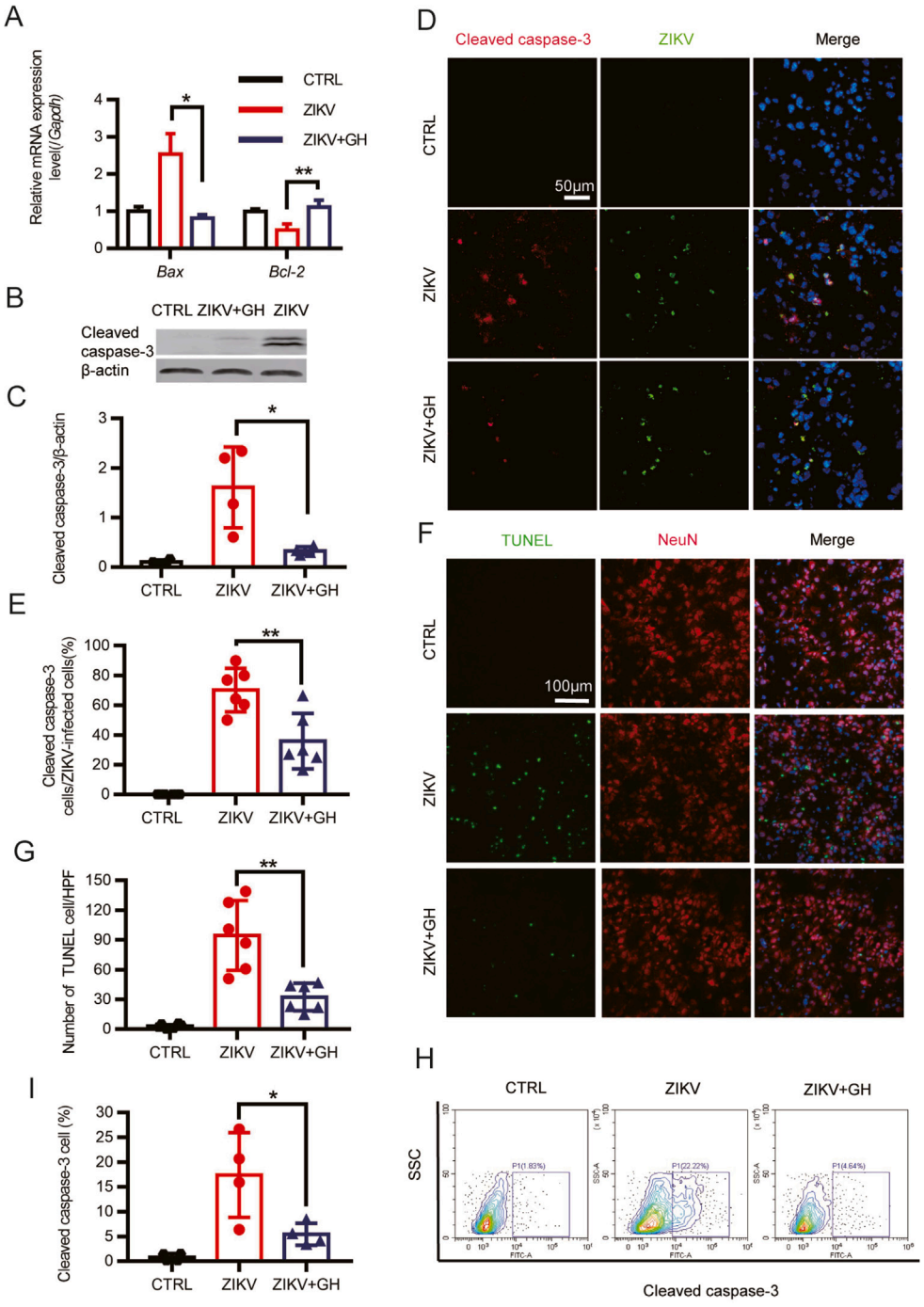

Fig. 5. GH alleviated the apoptosis of brain caused by ZIKV infection. **A** Relative expression of *Bax* and *Bcl*-2 mRNA in mouse brains at 7 dpi (CTRL n = 4, ZIKV and ZIKV + GH n = 6). **B** Immunoblotting detection of cleaved caspase-3 in brain at 9 dpi (n = 4 for each group). β-actin was used as control. **C** Quantification of the gray density of cleaved caspase-3 (n = 4 for each group). **D** Immunofluorescent co-staining of ZIKV antigens (green) and anti-cleaved caspase-3 (red) antibody in the brain at 9 dpi. DAPI (blue) denotes nucleus. **E** Percentage of cleaved caspase-3 positive cells in ZIKV-infected cells at 9 dpi. **F** Immunofluorescent co-staining of NeuN (red) and TUNEL (green). DAPI (blue) denotes nucleus. This image is the representative of ZIKV-infected and GH-treated mice. **G** Quantification of TUNEL positive cells per high power field (HPF). **H**, **I** Percentage of cleaved caspase-3 positive cells in cerebral cortex at 9 dpi analyzed by flow cytometry. The data are expressed as means ± SEM. Each dot denotes a mouse. $^{*}P < 0.05$, $^{**}P < 0.01$, as analyzed by student *t*-test. CTRL, control; GH, growth hormone; ZIKV, Zika virus; SEM, standard error of mean.

including the activation of the Ras-ERK pathway, and the blockade of the signaling pathway also led to a significant reduction in the effect of GH (Devesa et al., 2014). Therefore, we speculate that GH plays important roles in alleviation of ZIKV-induced damage in brain by regulating various signals and molecules.

In this study, it was found that GH inhibited cell apoptosis and inflammatory cell infiltration in the brain tissue of ZIKV infected mice. And GH has similar effects in suckling mice and adult mice. Although the survival rate of adult mice was not significantly improved after GH treatment, apoptosis and inflammatory cell infiltration in the brain tissue

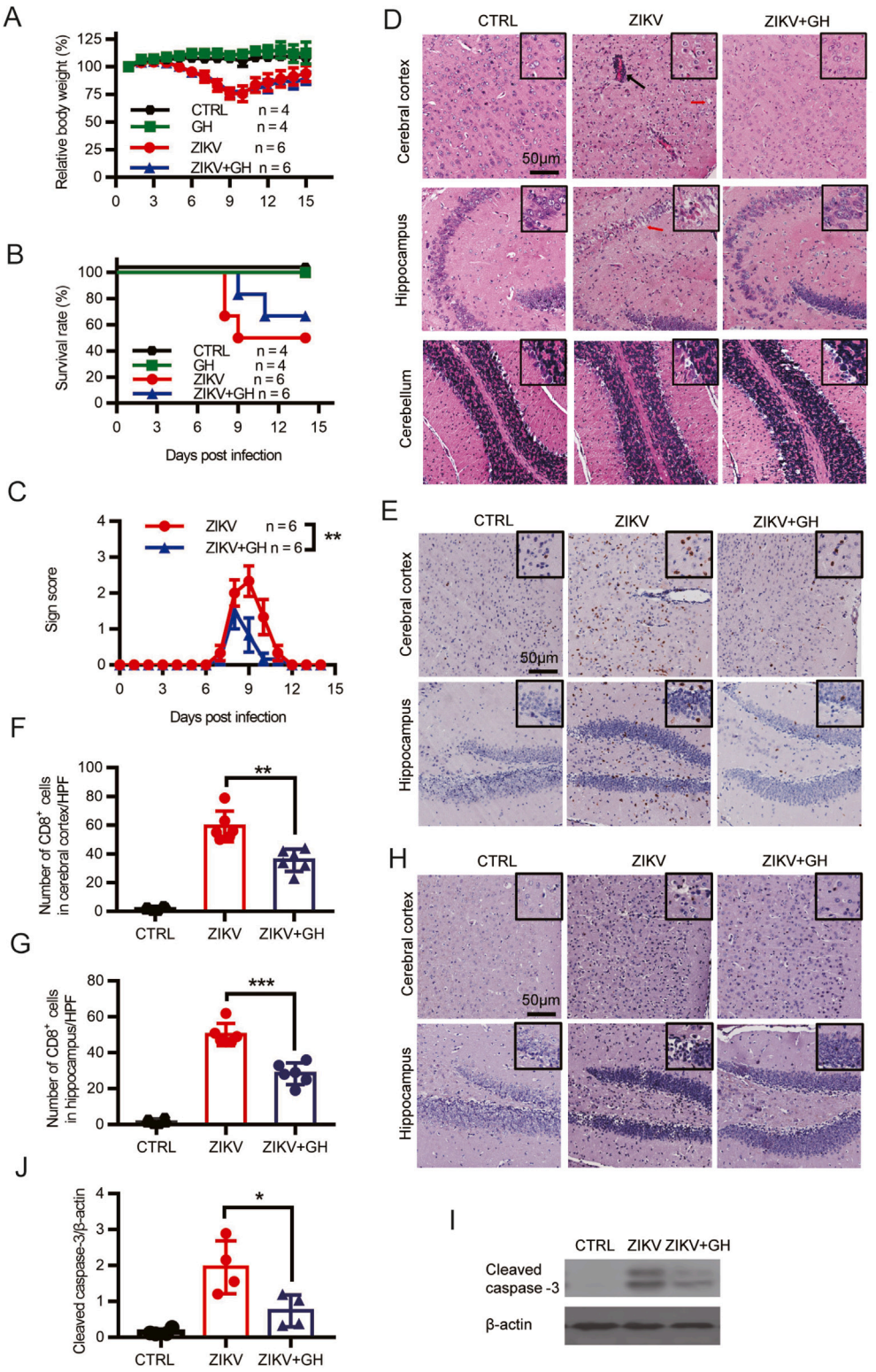

(caption on next page)

Fig. 6. Effects of GH on ZIKV-infected adult mice. **A** Changes of body weight of adult mice intraperitoneal injected with 2000 PFU ZIKV. GH was given daily for the first 7 days at 6 μg/g body weight (n = 6 for ZIKV and ZIKV + GH group, n = 4 for GH and CTRL group). **B** Survival rate of adult mice. **C** Sign score of ZIKV-infected adult mice (n = 6 for each group). **D** Hematoxylin eosin staining of cerebral cortex, hippocampus and cerebellum of adult mice at 9 dpi. Red arrows are cell loss, black arrows are inflammatory cell infiltration. Representative IHC image and count of $CD8^+$ T cells (**E–G**) and $CD4^+$ T (**H**) cells infiltration in brain at 9 dpi. **I** Immunoblotting detection of cleaved caspase-3 in brain at 9 dpi, and β-actin was used as control. **J** Quantification of the gray density of cleaved caspase-3, n = 4 for each group. Data are expressed as means ± SEM. Body weight was compared by two-way ANOVA. The survival curves were compared by log-rank test. Scores of the infection signs were compared by rank-sum test. Quantification of cleaved caspase-3 was compared by student *t*-test. $^{**}P < 0.01$, $^{***}P < 0.001$. CTRL, control; GH, growth hormone; ZIKV, Zika virus; SEM, standard error of mean.

of adult mice were also significantly reduced. Downregulation of GH receptor expression in the adult mouse nervous system may account for the insignificant overall protective effect of GH.

5. Conclusions

In summary, the data show that GH has a significant protective effect on ZIKV infected mice, especially in suckling mice. GH treatment improves growth retardation caused by ZIKV infection through inhibiting apoptosis and inflammatory cell infiltration in brain tissue. In addition, antenatal ZIKV exposure may lead to adverse infant outcomes including microcephaly and being small for gestational age, which are at high risk of adverse outcomes in the first year of life (Adachi et al., 2020). GH has been proven to be able to be used for treatment of small for gestational age children. The results provide important evidences not only for understanding the mechanism underlying ZIKV associated neurological symptoms but also for the treatment of ZIKV infection.

Data availability

All the data generated during the current study are included in the manuscript.

Ethics statement

All institutional and national guidelines for the care and use of laboratory animals were followed, and all the animal experiments were approved by the Experimental Animal Welfare and Animal Ethics Committee of Capital Medical University, Beijing, China (permission code: AEEI-2015–048; permission date: April 20, 2015).

Author contributions

Zi-Da Zhen: data curation, writing-original draft preparation. Na Wu: resources, conceptualization. Dong-Ying Fan: project administration. Jun-Hong Ai: methodology. Zheng-Ran Song: methodology. Jia-Tong Chang: methodology. Pei-Gang Wang: writing-reviewing and editing. Yan-Hua Wu: writing-reviewing and editing. Jing An: writing-reviewing and editing, supervision.

Conflict of interest

The authors declare that they have no conflict of interest.

Acknowledgements

This work was funded by the grants from the National Key Research and Development Plan of China (2021YFC2300200), the National Natural Science Foundation of China (NSFC) (U1902210 and 81972979 to J. An, and 82172266 to P.G. Wang) and Support Project of High-level Teachers in Beijing Municipal Universities in the Period of 13th Five-year Plan (IDHT20190510 to J. An).

Appendix A. Supplementary data

Supplementary data to this article can be found online at https://doi.org/10.1016/j.virs.2022.06.004.

References

Adachi, K., Romero, T., Nielsen-Saines, K., Pone, S., Aibe, M., Barroso de Aguiar, E., Sim, M., Brasil, P., Zin, A., Tsui, I., Gaw, S.L., Halai, U.A., Vasconcelos, Z., Pereira, J.P., Salles, T.S., Barbosa, C.N., Portari, E., Cherry, J.D., Pone, M., Moreira, M.E., 2020. Early clinical infancy outcomes for microcephaly and/or small for gestational age zika-exposed infants. Clin. Infect. Dis. 70, 2663–2672.

Aramburo, C., Alba-Betancourt, C., Luna, M., Harvey, S., 2014. Expression and function of growth hormone in the nervous system: a brief review. Gen. Comp. Endocrinol. 203, 35–42.

Cugola, F.R., Fernandes, I.R., Russo, F.B., Freitas, B.C., Dias, J.L., Guimaraes, K.P., Benazzato, C., Almeida, N., Pignatari, G.C., Romero, S., Polonio, C.M., Cunha, I., Freitas, C.L., Brandao, W.N., Rossato, C., Andrade, D.G., Faria Dde, P., Garcez, A.T., Buchpigel, C.A., Braconi, C.T., Mendes, E., Sall, A.A., Zanotto, P.M., Peron, J.P., Muotri, A.R., Beltrao-Braga, P.C., 2016. The brazilian zika virus strain causes birth defects in experimental models. Nature 534, 267–271.

Dang, J., Tiwari, S.K., Lichinchi, G., Qin, Y., Patil, V.S., Eroshkin, A.M., Rana, T.M., 2016. Zika virus depletes neural progenitors in human cerebral organoids through activation of the innate immune receptor tlr3. Cell Stem Cell 19, 258–265.

Devesa, P., Agasse, F., Xapelli, S., Almenglo, C., Devesa, J., Malva, J.O., Arce, V.M., 2014. Growth hormone pathways signaling for cell proliferation and survival in hippocampal neural precursors from postnatal mice. BMC Neurosci. 15, 100.

Ferraris, P., Cochet, M., Hamel, R., Gladwyn-Ng, I., Alfano, C., Diop, F., Garcia, D., Talignani, L., Montero-Menei, C.N., Nougairede, A., Yssel, H., Nguyen, L., Coulpier, M., Misse, D., 2019. Zika virus differentially infects human neural progenitor cells according to their state of differentiation and dysregulates neurogenesis through the notch pathway. Emerg. Microb. Infect. 8, 1003–1016.

Figueiredo, C.P., Barros-Aragao, F.G.Q., Neris, R.L.S., Frost, P.S., Soares, C., Souza, I.N.O., Zeidler, J.D., Zamberlan, D.C., de Sousa, V.L., Souza, A.S., Guimaraes, A.L.A., Bellio, M., Marcondes de Souza, J., Alves-Leon, S.V., Neves, G.A., Paula-Neto, H.A., Castro, N.G., De Felice, F.G., Assuncao-Miranda, I., Clarke, J.R., Da Poian, A.T., Ferreira, S.T., 2019. Zika virus replicates in adult human brain tissue and impairs synapses and memory in mice. Nat. Commun. 10, 3890.

Gabriel, E., Ramani, A., Karow, U., Gottardo, M., Natarajan, K., Gooi, L.M., Goranci-Buzhala, G., Krut, O., Peters, F., Nikolic, M., Kuivanen, S., Korhonen, E., Smura, T., Vapalahti, O., Papantonis, A., Schmidt-Chanasit, J., Riparbelli, M., Callaini, G., Kronke, M., Utermohlen, O., Gopalakrishnan, J., 2017. Recent zika virus isolates induce premature differentiation of neural progenitors in human brain organoids. Cell Stem Cell 20, 397–406 e395.

Gong, Y., Luo, S., Fan, P., Zhu, H., Li, Y., Huang, W., 2020. Growth hormone activates pi3k/akt signaling and inhibits ros accumulation and apoptosis in granulosa cells of patients with polycystic ovary syndrome. Reprod. Biol. Endocrinol. 18, 121.

Han, X., Wang, J., Yang, Y., Qu, S., Wan, F., Zhang, Z., Wang, R., Li, G., Cong, H., 2021. Zika virus infection induced apoptosis by modulating the recruitment and activation of pro-apoptotic protein bax. J. Virol. 95 (8) e01445-20.

Keane, J., Tajouri, L., Gray, B., 2015. The effect of growth hormone administration on the regulation of mitochondrial apoptosis in-vivo. Int. J. Mol. Sci. 16, 12753–12772.

Khaiboullina, S., Uppal, T., Kletenkov, K., St Jeor, S.C., Garanina, E., Rizvanov, A., Verma, S.C., 2019. Transcriptome profiling reveals pro-inflammatory cytokines and matrix metalloproteinase activation in zika virus infected human umbilical vein endothelial cells. Front. Pharmacol. 10, 642.

Lee, J.K., Kim, J.A., Oh, S.J., Lee, E.W., Shin, O.S., 2020. Zika virus induces tumor necrosis factor-related apoptosis inducing ligand (trail)-mediated apoptosis in human neural progenitor cells. Cells 9, 2487.

Li, C., Xu, D., Ye, Q., Hong, S., Jiang, Y., Liu, X., Zhang, N., Shi, L., Qin, C.F., Xu, Z., 2016. Zika virus disrupts neural progenitor development and leads to microcephaly in mice. Cell Stem Cell 19, 120–126.

Li, P., Jiang, H., Peng, H., Zeng, W., Zhong, Y., He, M., Xie, L., Chen, J., Guo, D., Wu, J., Li, C.M., 2021. Non-structural protein 5 of zika virus interacts with p53 in human neural progenitor cells and induces p53-mediated apoptosis. Virol. Sin. 36, 1411–1420.

Lindboe, J.B., Langkilde, A., Eugen-Olsen, J., Hansen, B.R., Haupt, T.H., Petersen, J., Andersen, O., 2016. Low-dose growth hormone therapy reduces inflammation in hiv-infected patients: a randomized placebo-controlled study. Inf. Disp. 48, 829–837.

Liu, B., Xu, Q., Wang, J., Lin, J., Pei, Y., Cui, Y., Wang, G., Zhu, L., 2019. Recombinant human growth hormone treatment of mice suppresses inflammation and apoptosis caused by skin flap ischemia-reperfusion injury. J. Cell. Biochem. 120, 18162–18171.

Liu, J., Li, Q., Li, X., Qiu, Z., Li, A., Liang, W., Chen, H., Cai, X., Chen, X., Duan, X., Li, J., Wu, W., Xu, M., Mao, Y., Chen, H., Li, J., Gu, W., Li, H., 2018. Zika virus envelope protein induces g2/m cell cycle arrest and apoptosis via an intrinsic cell death signaling pathway in neuroendocrine pc12 cells. Int. J. Biol. Sci. 14, 1099–1108.

Svensson, A.L., Bucht, N., Hallberg, M., Nyberg, F., 2008. Reversal of opiate-induced apoptosis by human recombinant growth hormone in murine foetus primary hippocampal neuronal cell cultures. Proc. Natl. Acad. Sci. U. S. A. 105, 7304–7308.

Tian, F.Y., Wu, B., Xu, T., Jiang, X.H., 2017. Systematic evaluation on effectiveness and safety of recombinant human growth hormone in treating adult patients with severe burn. Zhonghua Shaoshang Zazhi 33, 568–573.
Wang, J., Wu, J., Zhang, Y., Zhang, J., Xu, W., Wu, C., Zhou, P., 2021. Growth hormone protects against ovarian granulosa cell apoptosis: alleviation oxidative stress and enhancement mitochondrial function. Reprod. Biol. 21, 100504.
Wang, Z.Y., Wang, Z., Zhen, Z.D., Feng, K.H., Guo, J., Gao, N., Fan, D.Y., Han, D.S., Wang, P.G., An, J., 2017. Axl is not an indispensable factor for zika virus infection in mice. J. Gen. Virol. 98, 2061–2068.
Wu, Y.H., Cui, X.Y., Yang, W., Fan, D.Y., Liu, D., Wang, P.G., An, J., 2018. Zika virus infection in hypothalamus causes hormone deficiencies and leads to irreversible growth delay and memory impairment in mice. Cell Rep. 25, 1537–1547.e4.
Xu, D., Li, C., Qin, C.F., Xu, Z., 2019. Update on the animal models and underlying mechanisms for zikv-induced microcephaly. Annu Rev Virol 6, 459–479.
Zimmerman, M.G., Bowen, J.R., McDonald, C.E., Young, E., Baric, R.S., Pulendran, B., Suthar, M.S., 2019. Stat5: a target of antagonism by neurotropic flaviviruses. J. Virol. 93 e00665-19.